

Robust Fault-tolerant Control Using On-line Control Re-allocation with Application to Aircraft

Sijun Ye, Youmin Zhang, *Senior Member, IEEE*, Xinmin Wang, and C. A. Rabbath, *Senior Member, IEEE*

Abstract—This paper investigates the design problem of robust Fault-Tolerant Control (FTC) by using on-line control re-allocation for a class of uncertain systems and its application to flight tracking control. The design procedure consists of two parts: robust fault-tolerant baseline controller design, and realization of a control re-allocation scheme. The baseline controller is obtained by an iterative LMI method, which not only stabilizes the uncertain system but also provides sufficient robustness to allow for an effective operation of the Fault Detection and Diagnosis (FDD) subsystem in the event of actuator failures. The re-allocation scheme redesigns an optimal control law without requiring reconfiguration of the baseline controller, and compensates for actuator saturation via Cascaded Generalized Inverse (CGI) method. Simulation results show the effectiveness of the proposed approach.

I. INTRODUCTION

IT is well known that any control system will inevitably be subject to component failures such as actuator and/or sensor faults which can bring performance degradation, and even instability. This has ignited enormous research activities in Fault-Tolerant Control (FTC) with the objective of maintaining overall closed-loop system stability and acceptable performance in the event of such failures. Generally speaking, the FTC design approaches can be categorized into two main classes: passive [1]-[3] and active (see [4] and the references therein). The passive approach needs a prior knowledge of fault modes to obtain a fixed controller which is applied to both normal and fault cases. Therefore, the Passive FTC (PFTC) which does not require on-line Fault Detection and Diagnosis (FDD) and control reconfiguration, implements easier than Active FTC (AFTC). Nevertheless, PFTC yields more conservativeness as the number of presumed faults increase. On the contrary, AFTC compensates for component failures either by switching a set of pre-computed control laws or loading a new redesign control strategy on-line. It is obvious that the accurate system

state and parameters should be obtained for control reconfiguration by FDD. Unfortunately, there is very limited time available for FDD and control reconfiguration in the post-fault control system, especially for flight control of aerobatic and fighter aircraft.

To solve the above-mentioned problems of PFTC and AFTC, a new architecture for FTC System (FTCS) that includes a robust fault-tolerant baseline controller and on-line control re-allocation is proposed. Control Allocation (CA) is an approach to manage actuator redundancy for different control strategies handling actuator faults [5]-[9], [12], [14]. Recent works [5], [12] and [14] show that the effectiveness of control re-allocation methods for FTC when control surfaces are partially lost or jammed. However, these works neither focus on the design approach for the baseline controller nor investigate the effects of baseline controller to the performance of control re-allocation on FTCS.

In this paper, the robust baseline controller is achieved by an iterative LMI algorithm, which not only stabilizes the uncertain system but also provides sufficient robustness to allow more time to the computation of the FDD function in the event of actuator failures. Subsequently, an on-line control re-allocation scheme is designed based on the Pseudo-Inverse Method (PIM) and the Cascaded Generalized Inverse (CGI) method without requiring reconfiguration of the baseline controller. The novel FTCS including robust baseline controller and CA has been applied to the fully nonlinear ADMIRE fighter aircraft model.

II. PRELIMINARIES AND PROBLEM FORMULATION

To demonstrate the function and placement of the baseline controller and control re-allocation in the new FTCS, the general structure of the FTCS for flight tracking control is shown in Fig. 1.

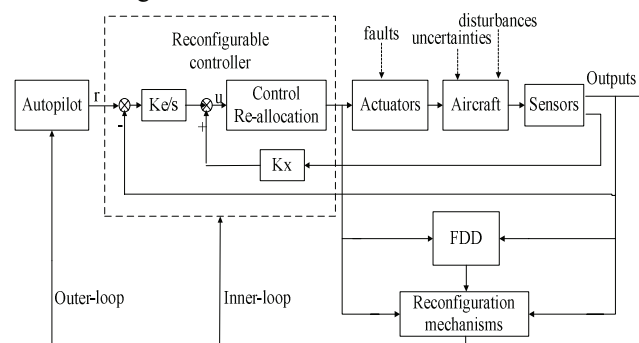


Fig. 1. General structure of the new FTCS.

S. J. Ye is with the School of Automation, Northwest Polytechnical University, Xi'an, Shaanxi, 710072, China and the Department of Mechanical and Industrial Engineering, Concordia University, Montreal, Quebec H3G 1M8, Canada (e-mail: yesijun@gmail.com).

Y. M. Zhang is with the Department of Mechanical and Industrial Engineering, Concordia University, Montreal, Quebec H3G 1M8, Canada (e-mail: ymzhang@encs.concordia.ca).

X. M. Wang is with the School of Automation, Northwest Polytechnical University, Xi'an, Shaanxi, 710072, China (e-mail: wxmin@nwpu.edu.cn).

C. A. Rabbath is with the Defence Research and Development Canada, Valcartier, Quebec G3J 1X5, Canada (email: camille-alain.rabbath@drdc-rddc.gc.ca).

Consider an uncertain linear time-invariant (LTI) system of the form

$$\begin{cases} \dot{x}(t) = [A + \Delta A(t)]x(t) + [B + \Delta B(t)]u(t) + [G + \Delta G(t)]w(t) \\ y(t) = Cx(t) \end{cases} \quad (1)$$

where $x(t) \in \mathbb{R}^n$ is the state, $u(t) \in \mathbb{R}^m$ is the control input, $w(t) \in \mathbb{R}^h$ is the disturbance input and $y(t) \in \mathbb{R}^p$ is the output. A, B, C and G are known real constant matrices with appropriate dimensions, which describe the nominal system. $\Delta A(t)$, $\Delta B(t)$ and $\Delta G(t)$ are real-valued time-varying matrix functions representing the norm-bounded parameter uncertainties.

$$\Delta A = E_a \Delta(t) F_a, \quad \Delta B = E_b \Delta(t) F_b, \quad \Delta G = E_g \Delta(t) F_g \quad (2)$$

where $\Delta^T(t)\Delta(t) \leq I$ [10].

Then, the system (1) with actuator faults is represented as:

$$\begin{cases} \dot{x}(t) = [A + \Delta A(t)]x(t) + [B + \Delta B(t)]\omega_L u(t) + [G + \Delta G(t)]w(t) \\ y(t) = Cx(t) \end{cases} \quad (3)$$

where ω_L is modeled by control effectiveness factors and satisfying

$$\begin{aligned} \omega_L &\in \Theta \quad \{\omega_L = \text{diag}[\omega_{L1}, \omega_{L2}, \dots, \omega_{Lm}], \\ &\omega_{Li} \in [\underline{\omega}_{Li}, \bar{\omega}_{Li}], \quad i = 1, 2, \dots, m\} \quad (4) \\ L &= 0, 1, \dots, 2^m - 1 \end{aligned}$$

For every fault mode, $\underline{\omega}_{Li}$ and $\bar{\omega}_{Li}$ represent the lower and upper bounds of ω_{Li} , respectively. Partial loss of control effectiveness is given by $0 < \omega_{Li} < 1$. $\omega_{Li} = 0$ means total outage of the i th actuator and $\omega_{Li} = 1$ denotes a healthy i th actuator.

Consider the autopilot command in Fig. 1 as a reference signal. The selected output $Sy(t)$ tracks the reference signal $r(t) \in \mathbb{R}^l$ without steady-state error, that is

$$\lim_{t \rightarrow \infty} e(t) = 0, \quad e(t) = r(t) - Sy(t) \quad (5)$$

where $e(t)$ is tracking error and $S \in \mathbb{R}^{l \times p}$ is a known constant matrix to select the output. It is well known that the tracking error integral action of a controller can effectively eliminate the steady-state tracking error [3]. In order to obtain a robust fault-tolerant controller with state feedback plus integral action of the tracking error, we restructure the system (3) as an augmented system based on the standard H_∞ -optimal tracking problem setting [3]. Then the state-space description of the augmented system is given by

$$\begin{aligned} \begin{bmatrix} e(t) \\ \dot{x}(t) \end{bmatrix} &= \begin{bmatrix} 0 & -SC \\ 0 & A + E_a \Delta(t) F_a \end{bmatrix} \begin{bmatrix} \int_0^t e(t) dt \\ x(t) \end{bmatrix} + \begin{bmatrix} 0 \\ B + E_b \Delta(t) F_b \end{bmatrix} \omega_L u(t) \\ &+ \begin{bmatrix} I & 0 \\ 0 & G + E_g \Delta(t) F_g \end{bmatrix} \begin{bmatrix} r(t) \\ w(t) \end{bmatrix} \quad L = 0, 1, \dots, 2^m - 1 \end{aligned} \quad (6)$$

Define the augmented state $\bar{x}(t) = [(\int_0^t e(t) dt)^T, x^T(t)]^T$ and disturbance $v(t) = [r^T(t), w^T(t)]^T$, then the augmented state

equation can be simplified as

$$\dot{\bar{x}}(t) = (\bar{A} + \bar{E}_a \bar{\Delta}(t) \bar{F}_a) \bar{x}(t) + (\bar{B} + \bar{E}_b \bar{\Delta}(t) \bar{F}_b) \omega_L u(t) + (\bar{G} + \bar{E}_g \bar{\Delta}(t) \bar{F}_g) v(t) \quad (7)$$

where

$$\begin{aligned} \bar{A} &= \begin{bmatrix} 0 & -SC \\ 0 & A \end{bmatrix}, \quad \bar{B} = \begin{bmatrix} 0 \\ B \end{bmatrix}, \quad \bar{G} = \begin{bmatrix} I & 0 \\ 0 & G \end{bmatrix}, \\ \bar{E}_a &= \begin{bmatrix} 0 \\ E_a \end{bmatrix}, \quad \bar{F}_a = [0 \quad F_a], \quad \bar{E}_b = \begin{bmatrix} 0 \\ E_b \end{bmatrix}, \quad \bar{F}_b = F_b, \\ \bar{E}_g &= \begin{bmatrix} 0 \\ E_g \end{bmatrix}, \quad \bar{F}_g = [0 \quad F_g], \quad \bar{\Delta}(t) = \Delta(t). \end{aligned}$$

Assumption 1: The state of the system (3) is available at every time instant.

In the following design, we choose a Linear Quadratic (LQ) performance index as:

$$J_L = \int_0^t [\bar{x}^T(t) Q \bar{x}(t) + u^T(t) R u(t)] dt \quad (8)$$

where $Q = \text{diag}[Q_1, Q_2] \in \mathbb{R}^{(l+n) \times (l+n)}$, $Q_1 \in \mathbb{R}^{l \times l}$ and $Q_2 \in \mathbb{R}^{n \times n}$ are symmetric positive semi-definite matrices and $R \in \mathbb{R}^{m \times m}$ is a symmetric positive definite matrix.

III. ROBUST FAULT-TOLERANT CONTROLLER DESIGN

In this section, we develop an iterative LMI algorithm to achieve a baseline controller such that:

- 1) the controller stabilizes the closed-loop augmented system in both normal and fault cases.
- 2) the controller minimizes the upper bounds of the LQ performance index given in (8).
- 3) the controller optimizes the performance of the closed-loop augmented system in the healthy case.

Consider the following state-feedback controller for the augmented system (7):

$$u(t) = K \bar{x}(t) = K_e \int_0^t e(t) dt + K_x x(t) \quad (9)$$

where $K = [K_e \quad K_x] \in \mathbb{R}^{m \times (l+n)}$.

Then, the closed-loop augmented system is represented as follows by substituting (9) into (7)

$$\begin{cases} \dot{\bar{x}}(t) = \{[\bar{A} + \bar{E}_a \bar{\Delta}(t) \bar{F}_a] + [\bar{B} + \bar{E}_b \bar{\Delta}(t) \bar{F}_b] \omega_L K\} \bar{x}(t) + [\bar{G} + \bar{E}_g \bar{\Delta}(t) \bar{F}_g] v(t) \\ z(t) = (C_1 + D_1 K) \bar{x}(t) \end{cases} \quad (10)$$

where

$$C_1 = [Q^{1/2}, 0]^T \in \mathbb{R}^{(l+n+m) \times (l+n)}, \quad D_1 = [0, R^{1/2}]^T \in \mathbb{R}^{(l+n+m) \times m},$$

and $z(t)$ is the required output.

Lemma 1 [10]: Given matrices Y, E and F of appropriate dimensions, where Y is symmetrical, and $\Delta^T(t)\Delta(t) \leq I$. Then

$$Y + E \Delta(t) F + F^T \Delta^T(t) E^T < 0 \quad (11)$$

holds if and only if there exists a scalar $\varepsilon > 0$ such that

$$Y + \varepsilon E E^T + \varepsilon^{-1} F^T F < 0 \quad (12)$$

Lemma 2 [15]: For a given positive scalar γ , if there exist symmetric positive definite matrix P satisfying

$$\begin{bmatrix} * & * & * & * & * \\ * & * & * & * & * \\ -R^{-1} & * & * & * & * \\ 0 & -\varepsilon_1^{-1}I & * & * & * \\ 0 & 0 & -\varepsilon_2^{-1}I & * & * \\ 0 & 0 & 0 & -\varepsilon_2 I & * \\ 0 & 0 & 0 & 0 & -\varepsilon_3^{-1}I \end{bmatrix} < 0 \quad (19)$$

$$\begin{bmatrix} Y & I \\ I & X \end{bmatrix} > 0 \quad (20)$$

Then we obtain initial controller gain $K_{opt}^0 = V_{0opt} X_{0opt}^{-1}$.

Step 2: Minimize[$\text{trace}(P_L)$] subject to $P_L > 0$ and (14) with $K = K_{opt}^0$, then we obtain P_{Lopt}^0 .

Step 3: Set iterative initial Lyapunov function matrices $P_L^0 = P_{Lopt}^0$. At the i th iteration, let $P_L^i = P_L^{i-1}$, $K_{opt}^i = K_{opt}^{i-1}$ and minimize[$\text{trace}(P_L^i)$] subject to $P_L^i > 0$ and (17).

Step 4: If $|\text{trace}(P_0^{i-1} - P_0^i)| < \lambda$ where λ is a given error tolerance, the calculated $K = K_{opt}^i$ is the optimal controller. Otherwise, let $i = i + 1$ and return to Step 3.

Remark 2: The conservativeness of Theorem 2 lies in the difference between $P_L - P_{L0}$. Algorithm 1 tries to find a sequence of the auxiliary variables such that the proposed difference is closed to zero. With this algorithm, the conservativeness can be reduced effectively.

IV. CONTROL RE-ALLOCATION DESIGN

Consider an uncertain closed-loop augmented system as:

$$\dot{\bar{x}}(t) = \bar{A}'\bar{x}(t) + \bar{B}'_u u(t) + G'v(t) \quad (21)$$

where $\bar{A}' = \bar{A} + \bar{E}_a \bar{\Delta}(t) \bar{F}_a$, $\bar{B}'_u = \bar{B} + \bar{E}_b \bar{\Delta}(t) \bar{F}_b$ and $G' = \bar{G} + \bar{E}_g \bar{\Delta}(t) \bar{F}_g$.

Suppose that the control actuators suffer partial loss or total outage of their effectiveness. The post-fault model of the system (21) is given by

$$\dot{\bar{x}}(t) = \bar{A}'\bar{x}(t) + \bar{B}'_{fu} u(t) + G'v(t) \quad (22)$$

where $\bar{B}'_{fu} = \bar{B}'_u \bar{Q}_L$.

Assumption 2: Rank $\bar{B}'_u = k_1 < m$ and rank $\bar{B}'_{fu} = k_2 < m$, i.e., \bar{B}'_u and \bar{B}'_{fu} do not have full column rank.

Based on Assumption 2, \bar{B}'_u and \bar{B}'_{fu} can be factorized as $\bar{B}'_u = \bar{B}'_q \bar{B}'$ and $\bar{B}'_{fu} = \bar{B}'_{fq} \bar{B}'$, respectively [8]. Then, the alternative system representations of (21) and (22) are given by

$$\dot{\bar{x}}(t) = \bar{A}'\bar{x}(t) + \bar{B}'_q q(t) + G'v(t) \quad (23)$$

and

$$\dot{\bar{x}}(t) = \bar{A}'\bar{x}(t) + \bar{B}'_{fq} q_f(t) + G'v(t) \quad (24)$$

where $q(t) = \bar{B}'_u u(t)$ and $q_f(t) = \bar{B}'_{fu} u_f(t)$. $q(t)$ and $q_f(t)$ are regarded as virtual control inputs corresponding to physical control inputs $u(t)$ and $u_f(t)$. To modern fighter aircraft, the

number of physical control inputs is greater than the number of virtual control inputs [12]. Hence, the required control moments can be redistributed to remaining healthy control surfaces by means of control re-allocation.

It is assumed that a baseline control input $u(t)$ for the healthy aircraft has been calculated based on the method proposed in Section III. It should be noted that the virtual control input $q(t)$ is determined by $u(t)$. Choose an appropriate output $z'(t) = C_z \bar{x}(t)$ to be used in the control re-allocation, then the actual rate of $z'(t)$ is presented as:

$$\dot{z}'(t) = C_z \dot{\bar{x}}(t) = C_z A' \bar{x}(t) + C_z B'_q q(t) + C_z G' v(t) \quad (25)$$

The choice of $z'(t)$ is not unique but a natural choice is $z'(t) = [p \ q \ r]^T$ where p , q and r describe the roll rate, pitch rate and yaw rate, respectively [7].

Suppose the desired virtual control input is $q_f(t)$ in post-fault system dynamic equations. Then the desired rate of $z'(t)$ would be

$$\dot{z}'_f(t) = C_z \dot{\bar{x}}(t) = C_z A' x(t) + C_z B'_{fq} q_f(t) + C_z G' v(t) \quad (26)$$

Subsequently, we seek the desired control input $u_f(t)$ that makes the right-hand side of Eq. (27) as close as possible to that of Eq. (28), namely,

$$C_z B'_{fq} q_f(t) \approx C_z B'_q q(t) \quad (27)$$

Thus the actual rate of $z'(t)$ will approximate to the desired rate of $z'_f(t)$, i.e. $\dot{z}'(t) \approx \dot{z}'_f(t)$. Then, the control input $u_f(t)$ can be determined by minimization of the following quadratic function:

$$\min_q J = \frac{1}{2} \{ [B'_{fq} q_f(t) - B'_q q(t)]^T C_z^T Q' C_z [B'_{fq} q_f(t) - B'_q q(t)] \} \quad (28)$$

subject to

$$u_{\min}(t) \leq u(t) \leq u_{\max}(t) \quad (29)$$

where Q' is a positive definite matrix of proper dimension. $u_{\min}(t)$ and $u_{\max}(t)$ are the lower and upper bounds of the control surface positions, respectively. An explicit solution can be obtained as follows from minimization of the above quadratic function in (29):

$$u_f(t) = [(C_z B'_{fq})^T Q' (C_z B'_q)]^{-1} (C_z B'_q)^T Q' C_z B'_q u(t) \quad (30)$$

The above control re-allocation method is generally referred to as PIM. However, control constraint (29) is not considered in early works of PIM. To handle the control constraint, a CGI algorithm [12] has been proposed for control re-allocation as follows.

Algorithm 2:

Step 1: An initial control law is computed by Eq. (30) without considering control constraint (29). If none of the elements in the solution is saturated, then stop and implement this control law.

Step 2: If any of the elements in the solution exceeds the position limitation of actuators, set that control channel at the

saturation position, and the effects at saturation are subtracted from the desired moment. Then, the rest of the desired moment are redistributed again to obtain a new control law by PIM.

Step 3: If none of the elements in the redesigned control law is saturated, the calculated control law is the optimal solution of control re-allocation. Otherwise, return to Step 2.

Remark 3: Using the above CGI algorithm, the moment demand of the saturated control surfaces is redistributed to the remaining ones. This function is very helpful to FTCS since the saturation of control surfaces is a prevalent problem in post-fault systems.

V. ADMIRE SIMULATIONS

In this section, a simulation of the ADMIRE model is used to test the effectiveness of the new FTCS and investigate the effects of baseline controller to the performance of control re-allocation on the overall system.

The ADMIRE model represents a single seated, single engine small fighter aircraft with a delta-canard configuration. The linear aircraft model has been obtained at Mach 0.22 and altitude 3000 m [13]. The state is $x(t) = [\alpha \ \beta \ p \ q \ r]^T$ and the tracking signals are α , β , p , where α is angle of attack (deg), β is sideslip angle (deg), p is roll rate (deg/s), q is pitch rate (deg/s), r is yaw rate (deg/s). The control surface deflection is $u(t) = [\delta_{rc} \ \delta_{lc} \ \delta_{roe} \ \delta_{rie} \ \delta_{lie} \ \delta_{loe} \ \delta_r]^T$, which describes the deflections (deg) of right and left canards, right outer and inner elevons, left inner and outer elevons, and rudder, respectively. For the considered flight case

$$A = \begin{bmatrix} -0.5432 & 0.0137 & 0 & 0.9778 & 0 & 0 & 0 \\ 0 & -0.1179 & 0.2215 & 0 & -0.9661 & 0 & 0 \\ 0 & -10.5130 & -0.9967 & 0 & 0.6176 & 0 & 0 \\ 2.6221 & -0.0030 & 0 & -0.5057 & 0 & 0 & 0 \\ 0 & 0.7075 & -0.0939 & 0 & -0.2127 & 0 & 0 \end{bmatrix},$$

$$B = \begin{bmatrix} 0.0035 & 0.0035 & -0.0318 & -0.0548 & -0.0548 & -0.0318 & 0.0004 \\ -0.0063 & 0.0063 & 0.0024 & 0.0095 & -0.0095 & 0.0024 & 0.0287 \\ 0.6013 & -0.6013 & -2.2849 & -1.9574 & 1.9574 & 2.2849 & 1.4871 \\ 0.8266 & 0.8266 & -0.4628 & -0.8107 & -0.8107 & -0.4628 & 0.0024 \\ -0.2615 & 0.2615 & -0.0944 & -0.1861 & 0.1861 & 0.0944 & -0.8823 \end{bmatrix},$$

$$G = [0.1254 \ 0 \ 0 \ 0.0068 \ 0]^T.$$

We introduce seven kinds of actuator faults into the design procedure of the baseline controller. Considering the worst situation for actuator failures, assume that the actuator is total outage, namely, the effectiveness factor of the actuator decreases to zero. Thus, every fault holds the following condition: one effectiveness factor $\omega_{Li} = 0$ and other six effectiveness factors $\omega_{Lj} = 1$, $j = 1, 2, \dots, 7, j \neq i$.

Select the following proper weighting matrices

$$Q = \text{diag}[20, 20, 20, 10, 10, 4, 1, 1],$$

$$R = \text{diag}[10, 10, 10, 10, 10, 10, 10].$$

The baseline controller gain is obtained by using Algorithm 1:

$$K_{LMI} = \begin{bmatrix} 1.2084 & 4.3835 & -0.5557 & -2.4480 & -2.1149 & 0.0710 & -1.3426 & 3.0637 \\ 1.3493 & -4.1083 & 0.7749 & -2.6652 & 1.6431 & -0.3157 & -1.4679 & -3.2651 \\ -0.5363 & -1.1907 & -1.1422 & 0.9573 & -0.3473 & 0.6352 & 0.5159 & 0.1831 \\ -0.9175 & 0.6898 & -0.9027 & 1.7684 & -1.2451 & 0.4421 & 0.8598 & 1.1042 \\ -0.6364 & -0.8931 & 0.7320 & 1.2975 & 1.2783 & -0.3978 & 0.5934 & -1.0978 \\ -0.2525 & 1.0786 & 0.9847 & 0.4206 & 0.2113 & -0.6539 & 0.2695 & -0.1967 \\ -0.0075 & 5.6239 & -0.8037 & 0.0142 & -3.8442 & -0.0890 & -0.0037 & 3.8532 \end{bmatrix}$$

Then we choose $B'_u = B'_q B'$, $B'_q = [0_{5 \times 3} \ I_{3 \times 3}]^T$, where B' includes the last three rows of B . The reconfiguration control law $u_f(t)$ with the re-allocation can be achieved via the approach described in Section IV. For comparison purposes, the standard LQR controller K_{LQR} is also obtained. To be close to the real system, we carry out our simulations by using the original nonlinear aircraft model of ADMIRE. In the simulations, we set 40% parameter uncertainties in the A matrix and 20% parameter uncertainties in the B and G matrices, and a vertical gust disturbance of 6 m/s.

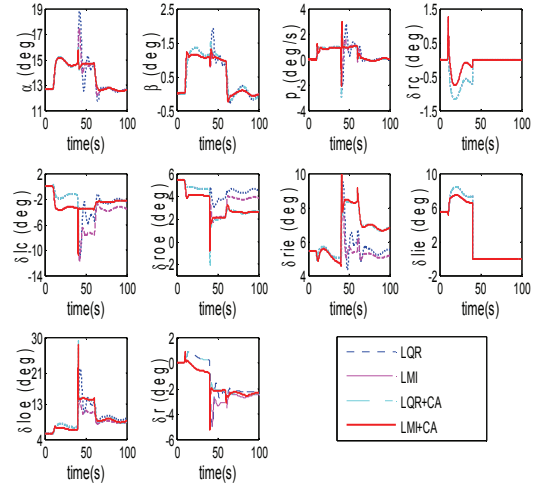


Fig. 2. Responses of output and control surface deflections to failures of right canard and left inner elevon.

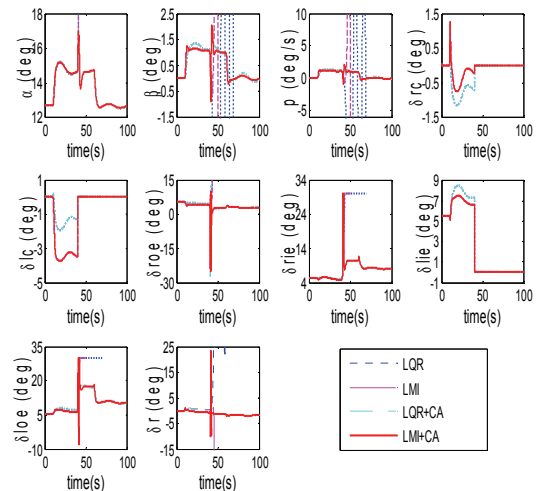


Fig. 3. Responses of output and control surface deflections to failures of right and left canards and left inner elevon.

VI. CONCLUSION

This paper proposed a novel FTCS which combines robust fault-tolerant controller and on-line control re-allocation for a class of uncertain systems. The robust fault-tolerant baseline controller stabilizes the uncertain system in both normal and fault cases, furthermore, provides sufficient robustness to achieve more time for FDD in the presence of actuator failures. The on-line control re-allocation scheme handles actuator failures directly and rapidly without requiring reconfiguration of the baseline controller. The simulation results of the nonlinear ADMIRE model demonstrate the advantages of the proposed FTCS.

REFERENCES

- [1] G. H. Yang, J. L. Wang, and Y. C. Soh, "Reliable H_∞ controller design for linear systems," *Automatica*, vol. 37, no. 5, pp. 717-725, 2001.
- [2] J. Chen, R. J. Patton, and Z. Chen, "An LMI approach to fault-tolerant control of uncertain systems," in *Proc. IEEE/ISIC/CIRA/ISAS joint Conference*, Gaithersburg, MD, pp. 175-180, 1998.
- [3] F. Liao, J. L. Wang, and G. H. Yang, "Reliable robust flight tracking control: An LMI approach," *IEEE Trans. Control Systems Technology*, vol. 10, no. 1, pp. 76-89, 2002.
- [4] Y. M. Zhang and J. Jiang, "Bibliographical review on reconfigurable fault-tolerant control systems," *Annual Reviews in Control*, vol. 32, no. 2, pp. 229-252, 2008.
- [5] H. Alwi and C. Edwards, "Fault tolerant control using sliding modes with on-line control allocation," *Automatica*, vol. 44, no. 7, pp. 1859-1866, 2008.
- [6] W. C. Durham, "Constrained control allocation," *J. Guidance, Control, and Dynamics*, vol. 17, no. 4, pp. 717-725, 1993.
- [7] M. Bodsan, "Evaluation of optimization methods for control allocation," *J. Guidance, Control, and Dynamics*, vol. 25, no. 4, pp. 703-711, 2002.
- [8] O. Harkegard and S. T. Glad, "Resolving actuator redundancy – optimal control vs. control allocation," *Automatica*, vol. 41, no. 1, pp. 137-144, 2005.
- [9] Y. Luo, A. Serrani and S. Yurkovich, "Model-predictive dynamic control allocation scheme for reentry vehicles," *J. Guidance, Control, and Dynamics*, vol. 30, no. 1, pp. 100-113, 2007.
- [10] L. H. Xie and C. E. de Souza, "Robust H_∞ control for linear systems with norm-bounded time-varying uncertainty," *IEEE Trans. Automatic Control*, vol. 37, no. 8, pp. 1188-1191, 1992.
- [11] K. M. Zhou, J. C. Doyle, and K. Glover, *Robust and optimal control*. Englewood Cliffs, NJ: Prentice-Hall, 1996.
- [12] Y. M. Zhang, V. S. Suresh, B. Jiang, and D. Theilliol, "Reconfiguration control allocation against aircraft control effector failures," in *Proc. 16th IEEE Int. Conf. on Control Application*, Singapore, pp. 1197-1202, 2007.
- [13] L. Forsell and U. Nilsson, "ADMIRE, the aero-data model in a research environment version 4.0, model description," FOI, Stockholm, Sweden, Technical Rep. FOI-R-1624-SE, 2005.
- [14] J. J. Burken, P. Lu, Z. L. Wu and, C. Bahm, "Two reconfigurable flight control design methods: robust servomechanism and control allocation," *J. Guidance, Control, and Dynamics*, vol. 24, no. 3, pp. 482-493, 2001.
- [15] S. P. Boyd, L. E. Ghaoui, E. Feron, and V. Balakrishnan, *Linear matrix inequalities in system and control theory*, SIAM Stud. Appl. Math. 15, SIAM, Philadelphia, 1994

Fig. 2 and Fig. 3 show the responses of the outputs and deflections of the control surfaces. In Fig. 2, when the actuators of the right canard and the left inner elevon are total outage at 40 seconds, the performance of two controllers without control re-allocation (LQR and LMI controllers) becomes unacceptable. Still, the LMI controller performs better than the LQR controller. The LQRCA controller (LQR controllers with control re-allocation) tracks the reference signal rapidly, but the steady-state tracking error is relatively large. It is obvious that the LMICA controller (LMI controllers with control re-allocation) results in superior system performance than the other controllers. In Fig. 3, when the actuators of the right and left canards and left inner elevon are total outage, the LQR and LMI controllers cannot stabilize the system. The LMICA and LQRCA controllers suffer from slight performance degradation. Therefore, as the number of actuator faults increases, the FTCS including the control re-allocation scheme yields better performance than the other systems.

In the above simulations, we assume that the actuator faults can be detected quickly, and set 40.5 seconds as threshold of control re-allocation. Unfortunately, we need more time to obtain accurate parameter estimates in a real system. Fig. 4 shows the responses of the desired output with the threshold increasing from 40.5 seconds to 41.5 seconds, and to 42.5 seconds. When the threshold is set at 40.5 seconds, we notice that the tracking performance of LQRCA controller is similar to that of LMICA controller from Fig. 4 (a). In Fig. 4 (b) and 4 (c), as threshold delays to 41.5 seconds and 42.5 seconds, the LQRCA controller yields unacceptable peak value and overshoot, and cannot stabilize the system. The LMICA controller just suffers from slight performance degradation. Consequently, the LMICA controller provides sufficient robustness so that the FDD has enough time to effectively perform.

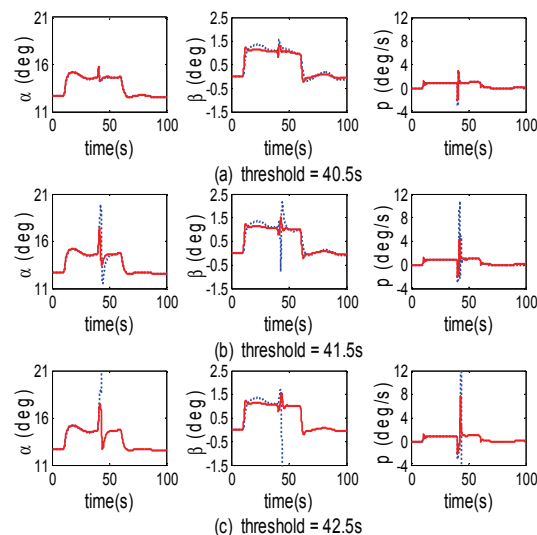


Fig. 4. Responses of output to different thresholds, where dotted line represents LQRCA controller and solid line represents LMICA controller.